Particle Accelerators, 1970, Vol. 1, pp. 121–136

THE PRINCIPLE OF SELF-COLLIDING ORBITS AND ITS POSSIBLE APPLICATION TO π–π AND μ–μ COLLISIONS†

ROBERT MACEK

Meson Physics Division, Los Alamos Scientific Laboratory, Los Alamos, New Mexico, USA

AND

BOGDAN MAGLIC‡

Department of Physics, Rutgers University, New Brunswick, New Jersey, USA

A principle for storage and collision of particles that are not available as targets is proposed; it provides interactions over the entire orbits of particles emitted with all crossing angles and momenta. The *self-colliding orbits* are achieved in a containing magnetic field in which the orbits *precess* about the center of symmetry which can also be the center of the production target. In the peripheral zone of the field, the momenta of positive and negative particles are antiparallel, thereby implying head-on collisions. All particles, regardless of their production angles, are eventually brought into this colliding zone by the virtue of their precession. This device, referred to as the 'Precetron', has a large momentum acceptance of pions, $\Delta p/p = 50\%$, and large angular acceptance, $\pm 180°$ in the horizontal and $\pm 10°$ in the vertical plane, in contrast to a conventional storage ring concept which would require well-defined momentum and small angular divergence. Single particle orbits have been calculated to first order; the precessing character of the orbits and the stability of the free oscillations are shown. Formulae for particle densities and luminosity in the colliding region have been derived for unstable particles. A Precetron with off-center target is also considered.

The construction of 'pion factories'[1–4] gives rise to the question of how far are we from observing real π–π and μ–μ collisions, such as

$$\pi^+ + \pi^- \to \pi^+ + \pi^- \quad \text{(a)}$$
$$\pi^+ + \pi^- \to \pi^\circ + \pi^\circ \quad \text{(b)}$$
$$\pi^+ + \pi^- \to 2\pi^+ + 2\pi^- \text{ etc.} \quad \text{(c)}$$

and

$$\mu^+ + \mu^- \to \mu^+ + \mu^- \quad \text{(d)}$$
$$\mu^+ + \mu^- \to e^+ + e^- \text{ etc.} \quad \text{(e)}$$

Csonka and Sessler[5] have discussed the use of the CERN intersecting storage ring for π–P and π–π scattering and Csonka[6] has considered other ideas.

The purpose of this paper[7] is to describe the principle for a particular storage-and-collision device which we call *Precetron*, because its operation is based on the collisions of particles whose orbits are constantly precessing. We calculate its characteristics and set forth the bounds for the primary (pion-producing) beam parameters needed to yield $\sim 10^4$ π–π collisions per hour.

While we also outline general methods for the detection of processes (a–e), detailed considerations of background difficulties and the experimental methods for separating processes (a–e) from the many possible processes are beyond the scope of this paper. It should be noted that backgrounds from π and proton collision with nuclei in the production target may greatly exceed the signal from π–π collisions. At this stage, however, our main concern is producing the necessary luminosity for reasonable unstable particle collision rates. We show how to produce and detect processes (a–e) but not how to discriminate against background. Nevertheless, we feel that presentation of our ideas at this time is useful because it describes a new method for particle storage and collision.

† Work supported in part by the United States Atomic Energy Commission under Contract AT(30-1) – 2171 while both authors were at the University of Pennsylvania.

‡ Supported by the National Science Foundation.

1. THE CONCEPT OF SELF-COLLIDING ORBITS

The geometry of the precessing orbits for particles which were emitted at the center of a radially decreasing magnetic field, is shown in Figs. 1a and 1b. An example of 'self-colliding orbits' of particles emitted from a point near the center is shown in Fig. 2. For particles of a given, fixed momentum we note that:

(1) Particles of the same mass but opposite charges precess in opposite directions with the same frequency regardless of their initial directions.

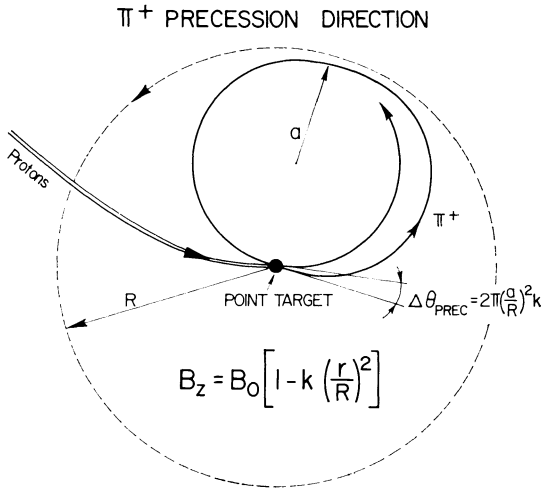

FIG. 1a. First turn for π^+ of median energy emitted at nearly 0° to the proton beam in a central target Precetron. The dashed line gives the direction of the π^+ orbit precession. B is directed into the plane of the paper; it is centered at the target and its radial dependence is given by $\propto 1-k\,(r/R)^2$, with $k=0.1$. The precession angle per revolution $\Delta\theta_{\text{prec}}$ is a function of the pion momentum (of its radius of curvature, a) and is equal to $2\pi\,(a/R)^2k$. The precession direction is always perpendicular to gradient of B.

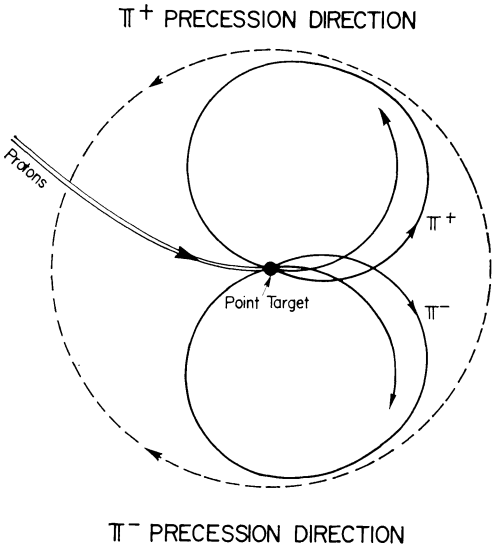

FIG. 1b. First turn for π^+ and π^- emitted at nearly 0° in a central Precetron. The two orbits will be on their collision course when $\Delta\theta_{\text{prec}}$ becomes $\sim 90°$.

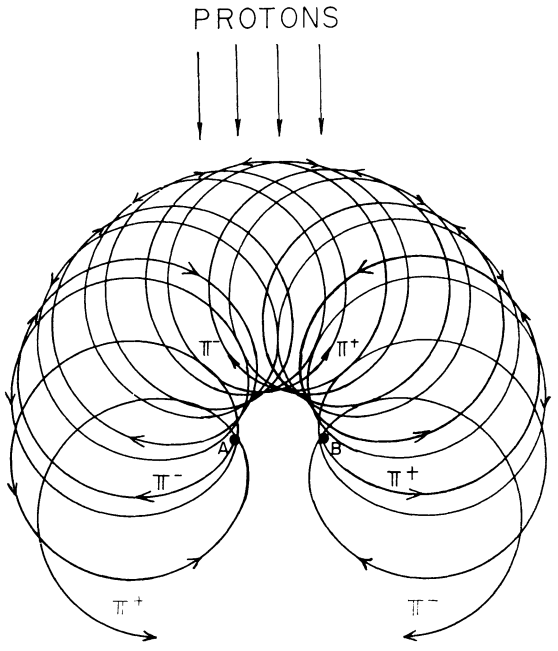

FIG. 2. Typical π^+ and π^- colliding orbits of *one* momentum; π^- and π^+ are emitted from points A and B, respectively, slightly displaced to the left and right of the field center. The points are separated in this drawing only for the illustration purpose; in principle, π^+ and π^- can be emitted from the same point.

(2) The particles collide over their entire precessing orbits. *All orbits*, regardless of the production angle, will eventually collide by the virtue of their precession; thus the horizontal angular acceptance is 360°.

(3) The highest density regions, with the most favorable crossing angles, are the extremely peripheral zone and the central zone (see Fig. 2); there, the momentum vectors of the positive and the negative particles are antiparallel thereby implying head-on collisions; we have considered only the peripheral zone in this study (see Sec. 3.3).

(4) The number of revolutions before decay of the unstable particle is independent of the particle momentum for constant B and is equal to $0.27\,B$ for pions and $30\,B$ for muons. Here B is the magnetic field in kilogauss. Since precession occurs only for nonuniform fields, the number of revolutions is only approximately independent of momentum.

For comparison, a scheme for pion-pion *colliding beams* or 'colliding rings' is shown in Figs. 3a and b. By the very definition of 'beam',

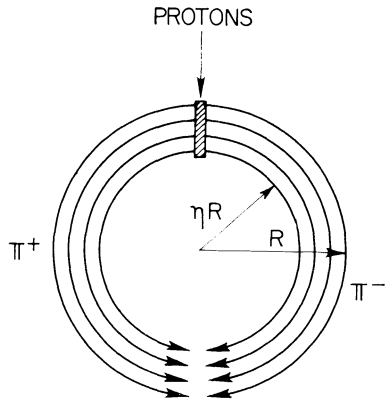

FIG. 3a. A scheme of a conventional colliding beam device with one proton beam striking the target in magnetic field and π^+ and π^- emitted at 90° are captured into orbits. The high-energy pion production at 90° is 2 orders of magnitude below that one in the region 0°–45°. For a large angular acceptance the 'beam' system becomes the 'offset Precetron', shown in Fig. 10.

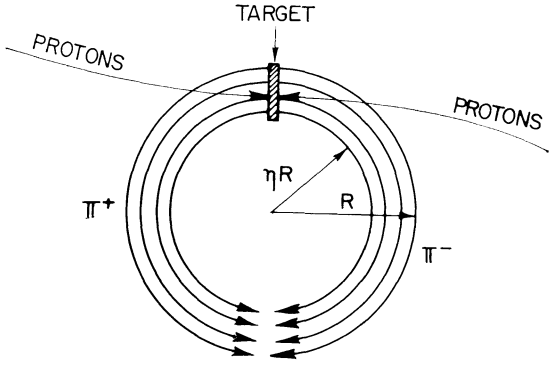

FIG. 3b. A scheme of a conventional colliding beam device with *two* proton beams striking the target in opposite directions and the π^+ and π^- emitted at 0° are captured into orbits.

the particle acceptance of the ring system is limited to nearly parallel rays, i.e., 0° ± small $\Delta\theta$, where $\Delta\theta \leqslant 10^{-2}$ or $\Delta\Omega \leqslant 10^{-4}$. In contrast, a device based on *self-colliding orbits* has an acceptance as large as $0° \pm 180°$ because of property (2). The solid angle is limited only by the finite vertical angular acceptance and can be of the order $\Delta\Omega \simeq 1$ sr. Thus, the *Precetron* captures $\sim 10^3$ to 10^4 times more colliding particles than the conventional ring. Since the luminosity is proportional to the square of the particle density, the precetron action results in the increase of luminosity by a factor 10^6 to 10^8, which is only slightly offset by our factor $\bar{\lambda}^2$ which accounts for the fact that only the particles in the peripheral zone have the crossing angles favorable for the collisions.

It should be pointed out that we have contrasted here two extreme cases: the beam in the usual sense (particles streaming in a well defined direction) and the Precetron with the target in the center, which contains particles moving in all directions. Obviously there is a continuum of intermediate cases. As one increases the angular acceptance of the beam in Figs. 3a and b, the precession of the orbit becomes more and more significant and the 'beam' takes the character of the Precetron. Hence, the beam systems in Figs. 3a and b, for a large angular acceptance becomes an 'Offset Precetron' shown in Fig. 10 and discussed in Sec. 6.

First, in Sec. 2, we shall derive the formula for the π–π luminosities obtainable with the obvious colliding beam schemes like the ones in Figs. 3. Next, in Sec. 3, we derive the luminosity formulae for the central Precetron in two ways: (1) intuitively, from the geometry of the orbits and (2) more exactly, by calculating particle densities.

2. FORMULAE FOR COLLIDING BEAMS OF UNSTABLE PARTICLES

2.1. *Interaction rate*

In describing colliding beam machines the concept of luminosity L, is defined in terms of the instantaneous reaction rate, I, and reaction cross section, σ, through

$$I = \sigma L \tag{1}$$

for any system. The average interaction rate $\bar{I}$, then, is the time average of I over an interval $t_2 - t_1$, and leads to an average luminosity $\bar{L}$ given by

$$\bar{L} = \frac{1}{t_2 - t_1} \int_{t_1}^{t_2} L(t)\, \mathrm{d}t \tag{2}$$

$$\bar{I} = \sigma \bar{L} \tag{3}$$

2.2. *Luminosity for colliding beam systems involving unstable particles*

Let us consider the schemes in Figs. 3a (or b) in which one (or two) proton beam(s) strike a target and produce π^+ and π^- beams symmetrically. If the π's spent all of their time in circular beams moving in opposite directions with 100 per cent overlap and zero crossing angles, the instantaneous luminosity would be:

$$L = 2\beta c \frac{n_+(t) n_-(t)}{V} \tag{4}$$

The factor 2 is the usual colliding beam factor which arises from two beams sweeping past one another.

The quantitities n^+ and n^- are the total number of π^+ and π^- respectively which are functions of time;

β_{+-} = the $\pi^+\pi^-$ relative velocity;
c = speed of light;
V = volume of the interaction region

V can be expressed as

$$V = \pi R^2(1-\eta^2)\,\Delta z \tag{5}$$

where R is the outside radius of the beam, ηR, the inside radius of the beam and Δz is its vertical extension. Equation (5) is approximately given by:

$$V \simeq 2\pi\bar{R} \times (\text{area}) \tag{6}$$

where $\bar{R}$ is the average radius of the beam. By 'area' we understand the cross-sectional area. Let us denote by κ the π^-/π^+ production ratio:

$$\kappa = n_-/n_+ \tag{7}$$

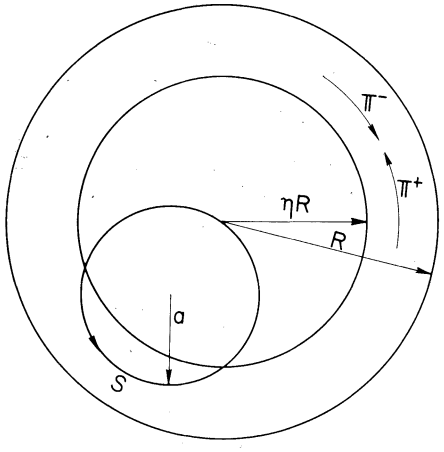

FIG. 4. One circular π orbit showing the shell from which the interactions are accepted. The shell is the region of radii from ηR to R. No precession is shown.

e.g. for 15° emission from 800 MeV protons on beryllium, $\kappa \cong 4.5^{-1}$. Further let us call f_+ the fraction of protons that are 'transformed' into the useful π^+'s, i.e. the pions that are captured into the colliding orbit, namely

$$n_+ = f_+ N_P, \tag{8}$$

where N_P = number of protons hitting the target. The fraction f is calculated from

$$f = \int \frac{\partial^2\sigma}{\partial\Omega\,\partial P}\,\mathrm{d}\Omega\,\mathrm{d}P\,\frac{T}{A}\,N_0 \tag{9}$$

where T = target length and A = atomic number of the target. With the substitution:

$$H = \frac{2\beta_{+-}c\kappa}{\pi R^2(1-\eta^2)\,\Delta z}, \tag{10}$$

the instantaneous luminosity becomes:

$$L = Hn_+^2 = Hf_+^2 N_P^2. \tag{11}$$

2.3. *Time-dependent luminosity for decaying particles*

Let us calculate $n(t)$ during and after a uniform proton burst. Figure 5 graphically depicts the time structure under consideration. We assume that it will not be possible to run with detectors turned on during the proton spill because of the background, so that detectors will be turned on only at the end of it.

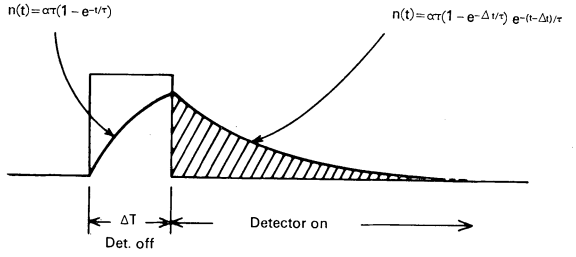

FIG. 5. Pion intensity as a function of time. ΔT = length of the proton spill onto the target inside the pot; τ = laboratory pion lifetime.

When the protons are hitting the target (detectors *off*), the pion intensity builds up according to:

$$n(t) = (\partial n/\partial t)\,\tau(1-e^{-t/\tau}) \tag{12}$$

where τ is the laboratory lifetime of the pion,

$$\tau = \gamma\tau_0, \tag{13}$$

and $\partial n/\partial t$ = instantaneous π-production rate which is proportional to the proton current, $\mathrm{d}N/\mathrm{d}t$;

$$\partial n/\partial t = f\frac{\mathrm{d}N}{\mathrm{d}t} \tag{14}$$

where f is given by Eq. (9).

Protons stop hitting the target after a time Δ. and the detectors are switched *on*. Then we have

$$n(t) = (\partial n/\partial t)\tau\,(1-e^{-\Delta t/\tau})\,e^{-(t-\Delta t)/\tau} \tag{15}$$

where Δt is the length of the proton burst and t any time after the beginning of the burst.

To compute the time average luminosity, $\bar{L}$, we need the time average of n^2. We assume that the

separation in time between two bursts is much larger than the burst length Δt so that

$$\bar{n}^2 = b \int_{\Delta t}^{\infty} n^2(t)\,dt \tag{16}$$

where b is the burst rate. After integration of (16) we obtain

$$\bar{L} = \tfrac{1}{2}\tau^3 H \left(\frac{\partial n}{\partial t}\right)^2 (1 - e^{-\Delta t/\tau})^2 b. \tag{17}$$

The instantaneous pion production rate, $\partial n/\partial t$, can be expressed as

$$\left(\frac{\partial n}{\partial t}\right) = \frac{fN_P}{b\Delta t} \tag{18}$$

In collisions of unstable particles, everything happens within the lifetime of the particles. Thus, all times should be expressed in units of the pion lifetime in the laboratory, τ, Eq. (13). If we denote the ratio of the burst length to the laboratory pion life time by g,

$$g = \Delta t/\tau, \tag{19}$$

Eq. (17) becomes:

$$\bar{L} = \tfrac{1}{2}\tau H (fN/bg)^2 (1 - e^{-g})^2 b \tag{20}$$

or

$$\bar{L} = \tfrac{1}{2}\tau H f_P^2 N_P^2 G \tag{21}$$

where the factors involving the time-structure of the beam are combined into G given by

$$G = \left(\frac{1 - e^{-g}}{g}\right)^2 \frac{1}{b} \tag{22}$$

If the original proton intensity is split into two beams as in the scheme of Fig. 2, then $N_P^2 \to \frac{1}{4} N_P^2$.

Nonpulsed detector regime. If the detectors can operate all the time including the spill time Δt, the integration of Eq. (16) is carried out from 0 to ∞. This results in approximately $2g$ times higher luminosity (for large values of g) than that given by Eqs. (21)–(22) because G becomes:

$$G = \frac{2}{bg}\left[1 - \left(\frac{1 - e^{-g}}{g}\right)\right], \tag{23a}$$

or

$$G = \frac{2}{bg} \quad \text{as} \quad g \to \infty. \tag{23b}$$

2.4. *Considerations of the primary beam structure*

From Eqs. (21)–(22) we see that for a fixed number of protons per second, N, the luminosity is best for the poorest duty cycle of the pion-producing beam. $\bar{L}$ is maximum when G has a maximum. Referring to Eq. (22), one can see that G has a broad maximum for a narrow burst, i.e., as $g \to 0$, $G \to 1/b$. The number of bursts, b, for a given average proton intensity should be as small as possible, hence the duty cycle, which can be written as

$$\text{Duty Cycle} = bg\gamma\phi\tau_0, \tag{24}$$

should be as small as possible. In other words, a high *instantaneous* intensity of π's produced per second, is desired. Obviously, it is advantageous to produce them in one burst of the order of magnitude of the laboratory pion lifetime.

Proton storage ring. An alternate solution to decreasing the linac's duty cycle has been suggested by D. Nagle (Priv. Comm.). The protons from a number of linac pulses are collected into a storage ring and then dumped in one short pulse. With this procedure one could obtain $b = g \simeq 1$ if protons can be stored in a ring of radius $r = 300$ cm and switched out in one turn ($\sim 10^{-7}$ sec). Proton injection into storage ring may be facilitated by using the 100 μA H^--beam at LAMPF. The 800 MeV H-ions can be converted to 800 MeV protons with very thin stripping foils.

Luminosity independent of pion momentum. Referring to Fig. 3, where four orbits, corresponding to four pion momenta, are drawn, we note that the number of revolutions before the pion decay is independent of the pion momentum p for a fixed value of the magnetic field B and the fixed cross-sectional area of the beam. This is easily seen by using the relation for the radius of curvature in the magnetic field B

$$R = \frac{p^{(\mathrm{MeV/c})}}{0.3\,B(\mathrm{kG})} = \frac{\gamma\beta m}{0.3\,B} \tag{25}$$

(m = pion mass in MeV) and substituting it in the following relation

$$\text{Number of revolutions} = \frac{\beta c\gamma\tau_0}{2\pi R} = \frac{0.3 c\tau_0 B}{2\pi m} \tag{26}$$

which gives 0.27 B revolutions.

Since the number of interactions is proportional to the number of revolutions of the colliding partners, the luminosity is also nearly independent of the momentum for B = const. and a constant cross-sectional area of the colliding beams. This can be shown by rewriting the product τH in Eqs. (20), (21) using

$$\tau = \gamma\tau_0 = \frac{p\tau_0}{\beta m} \tag{27}$$

Eq. (25) and Eq. (6). Then, Eq. (10) becomes:

$$\tau H = \frac{\gamma\tau_0\beta_{+-}c\kappa}{\pi R \times (\text{area})} = \frac{0.3\tau_0 c\kappa B}{\pi m \times (\text{area})}. \tag{28}$$

We have assumed $\beta_{+-} = \beta$ which is not quite correct. For constant B, any gain in the lifetime is compensated by the increase of the radius.

Luminosity proportional to B^3. It can be easily shown that the luminosity is proportional to the third power of the magnetic field B for p = const. This can be intuitively understood from the fact that L is inversely proportional to the interaction volume V [Eq. (4)], the latter scales like $1/B^3$ for a fixed configuration.

This can be shown more directly from Eq. (5) and noting that, for a given vertical angular acceptance Δz is directly proportional to R, as shown later in our consideration of particle orbits. Thus $V \propto R^3$ and with Eqs. (10) and (25), $L \propto B^3$.

3. PRECETRON: FORMULAE FOR SELF-COLLIDING ORBITS

3.1. *Simple model*

The simple model treats the narrow outer zone in Fig. 2, where the crossing angles are small, as two colliding beams. We can apply Eq. (4) to the Precetron by replacing n_+ and n_- by $n_+\bar{\lambda}$ and $n_-\bar{\lambda}$ where $\bar{\lambda}$ is the average fraction of the time a π is in the outer shell. This is no more than saying that the number of π's in the shell is the total number of π's times the probability that the π is in the shell.

We now list all the important assumptions of our simple model:

(a) A point target.

(b) A uniform particle distribution in the vertical (z) direction.

(c) A uniform momentum distribution over the region of interest.

(d) A π-production angular distribution which is isotropic to 45° then zero to 180°, also $\pi^-/\pi^+ = \kappa$.

(e) We will only consider interactions from the region with orbit diameters from ηR to the maximum diameter, R. We will assume that the crossing angles are approximately zero in this region.

(f) We will assume that the particle density is uniform in the region of interest. Later, in Sec. 3.2, we calculate the luminosity using the actual particle density distribution.

(g) A proton spill of duration Δt comparable to or longer than the precession period so that the Precetron is uniformly filled with the orbits and steady state collision rates can be calculated.

In Fig. 4 we show schematically the region of interest which is the outer shell from ηR to R. Also shown are typical orbits which reach the shell from which we accept interactions. In this shell the π's are moving mainly along the circumference of circles whose centers are at the target. In the shell the π's effectively become two currents of opposite charge moving in opposite directions around the target.

For the orbit in Fig. 4, λ is the ratio of the arc length S to the total perimeter of the orbit, i.e.,

$$\lambda(a) = \frac{S(a)}{2\pi a} \tag{28}$$

and

$$\bar{\lambda} = \int_{\eta R/2}^{R/2} \lambda(a) q(a)\, \mathrm{d}a \tag{29}$$

where $q(a)$ is the distribution of orbit radii (uniform) corresponding to the assumed momentum distribution.

From a simple consideration of this geometry in Fig. 4 we see that

$$S(a) = 4a \cos^{-1}\frac{\eta R}{2a} \tag{30a}$$

or

$$\lambda(a) = \frac{2}{\pi}\cos^{-1}\frac{\eta R}{2a}. \tag{30b}$$

It should also be noted that $\pi\lambda(a)$ is the maximum crossing angle for two orbits of radius a, intersecting inside the shell. For two orbits of radius a which intersect at a distance r from the origin, the crossing angle α is

$$\alpha = 2\cos^{-1}\frac{r}{2a}. \tag{31}$$

In general, two orbits of radii a_1 and a_2, intersecting at r have a crossing angle of

$$\alpha = \cos^{-1}\frac{r}{2a_1} + \cos^{-1}\frac{r}{2a_2}. \tag{32}$$

Using (30) for λ we obtain for $\bar{\lambda}$

$$\bar{\lambda} = \frac{2}{\pi}\int_{\eta R}^{R} \cos^{-1}\left(\frac{\eta R}{X}\right)\frac{\mathrm{d}x}{R(1-\eta)}$$

$$= \frac{2}{\pi}\frac{\eta}{1-\eta}\left[\frac{1}{\eta}\cos^{-1}\eta - \log\left(\frac{1+\sqrt{1-\eta^2}}{\eta}\right)\right]. \tag{33}$$

We are now ready to write down the Precetron luminosity, L_{PREC}, by introducing the basic assumption of our model

$$n_\pm \to \bar{\lambda} n_\pm \tag{34}$$

into the expression for the colliding beam luminosity, L, Eq. (11). This gives

$$L_{\mathrm{PREC}} = \bar{\lambda}^2 L, \tag{35}$$

with the $\bar{\lambda}$ given by Eq. (33). For $\eta = \frac{1}{2}$ we have $\bar{\lambda} = 0.49$. Hence, the Precetron luminosity with $\eta = \frac{1}{2}$ is about $\frac{1}{4}$ of the usual colliding beam luminosity with the same number of pions. However, the pion intensity is several order of magnitudes (10^3 to 10^4) times higher in the Precetron and the luminosity is proportional to the square of the intensity.

3.2. *Precetron luminosity using density calculation*

In Appendix B we derive a similar formula for this same model except that we calculate the actual particle densities D_+, D_- as functions of position. The average luminosity is obtained from

$$L = \int_{\text{shell}} 2\beta_{+-} c D_+ D_- d(\text{vol}) \qquad (36)$$

assuming a constant cross section over the range of center-of-mass energies included in the region of interaction. The result is formula (35) with a different expression for $\bar{\lambda}(\eta)$ given by Eq. (B. 13). Here we obtain $\bar{\lambda} = 0.58$ for $\eta = \frac{1}{2}$.

In Appendix B we also calculate the case where the momentum distribution is peaked about the average value and for a shape approximating π production data. Once again formula (35) is obtained but with a different expression for $\bar{\lambda}$. In this case $\bar{\lambda} = 0.85$ for $\eta = \frac{1}{2}$ [Eq. (B.19)].

The quantity $\bar{\lambda}$ in this case, unlike that in Sec. 3.1, is not computed as the fraction of time a pion spends in the shell. It is the factor that allows the luminosity to be written in the form of Eq. (35).

3.3. *Luminosity in the central zones of the Precetron*

The highest π–π collision rates will be near the target because pion density is largest there, but we have excluded this region because of two complications:

(a) Interactions of pions with the target will produce a background of pion pairs, which will exceed the real π–π scattering by many orders of magnitude and will not be distinguishable from it.

(b) The scattered π^+ and π^- cannot come out of the Precetron field from the central zones except for those more or less along the field direction.

Hence results computed in Secs. 3.1 and 3.2 are a *lower limit* on the luminosity.

4. PRECETRON ORBIT CALCULATIONS

We have investigated the single particle orbits in a weak focusing field approximately given by $B_z = B_0[1 - k(r^2/R^2)]$ where k is small, of order 0.1, and R is a radius of the magnetic field. The average field index is related to k by the relation $\bar{n} = (2a/R)^2 k$, so that for the largest orbit, $2a = R$, k is equal to the normal field index 'n'. Details are presented in Appendix A.

These calculations indicate that to first order the radial and vertical oscillations are stable, and the orbits precess about the z axis, with a precession frequency $k'/4$ times the orbital frequency where $k' = \bar{n} = (2a/R)^2 k$ and a is the radius of orbit.

Precessing single particle orbits for π^+ and π^- are shown in Figs. 1a, b, and 2. For a uniform proton spill, Δt, comparable or longer than the precession period, we will have a uniform azimuthal distribution of orbit centers.

In a shell near the outer envelope of the particle trajectory in Fig. 2 the particle is effectively providing a counter-clockwise current of say π^+'s. The π^- of the same momentum will move in the opposite direction and, in the outer shell, will be on a direct collision course with π^+ so that the crossing angle is approximately zero. The shell thickness can be a reasonable fraction of the orbit radius without containing large crossing angles. The particle density calculations for such precessing orbits are given in Appendix B.

5. PRECETRON: APPLICATION TO π–π AND μ–μ COLLISIONS

5.1. *The setup*

We consider the following setup: a solid metal target is placed in the center of a high magnetic field which is shaped to contain at least 100 turns of pions of momentum in the range $P_\pi = 310$–550 MeV/c $T_\pi = 200$–430 MeV). We assume a magnetic field of 400 kG (probably a pulsed one) which gives a radius 3.3 cm for the pion orbit of an average energy $\bar{T}_\pi = 300$ MeV ($\bar{P}_\pi = 415$ MeV/c).

The pions are produced by a proton beam incident onto the target which is $\sim$2 cm thick in the beam direction and narrow ($\sim$0.2 cm). In addition to pions, particles such as protons, deuterons and other light nuclei will also be produced and captured in the magnetic field. Later on, after one pion life-time, leptons will be present in the mixture, too. We shall refer to this early mixture of positive and negative orbits of various hadrons with different crossing angles and momenta as the *hadron jumble*, in contrast to the *lepton jumble* that will be orbiting later.

We believe that a pulsed, iron-free field capable

of containing the jumble can be produced by an appropriate coil configuration, and that a gap could be made about the midplane to allow exit of reaction products. Such a 'magnetic pot' could be accomplished by a pair of coils with the current in both in the same direction or by a more refined combination containing two pairs of coils of different radii and current. This point is covered in Appendix A.

5.2. *Identification of $\pi^+\pi^-$ collision products from the hadron jumble*

Let us consider the reaction

$$\pi^+ + \pi^- \to \pi^+ + \pi^-. \tag{37}$$

In P-wave scattering (rho meson), the angular distribution is strongly peaked forward and backward equally. The π's scattered forward are unlikely to leave the pot since they will tend to be recaptured in quasi-stable orbits. However, the *backward scattered pions* will be immediately kicked out of the field by the change of sign of the $\mathbf{v}\times\mathbf{B}$ force. Particles scattered more or less in the direction of the major component of the field will also exit. Thus, a reasonable fraction, of order half of the collisions, will be detectable.

The concurrent reaction

$$\pi^+ + \pi^- \to \pi^\circ + \pi^\circ \tag{38}$$

is obviously easier to detect regardless of the production angle. However, it can occur only from $I = 0$. This excludes the P-wave (ρ meson) whose cross section is believed to be dominant by an order of magnitude over the nonresonant (I = even) cross section.

The products of the π–P scattering will come out of the pot in a similar way; the discrimination of pions from protons can be done in a standard way. The calibration of the system might be done by using the π–P resonance.

The effective mass of the pion-pion or pion-proton pair is measured by the magnetic analysis of their momenta outside the pot, with conventional wide gap magnets surrounding it. The invariant quantity $M^2_{\pi^+\pi^-} = (E_+ + E_-)^2 - (\mathbf{p}_+ + \mathbf{p}_-)^2$ is independent of the energies and crossing angles of π^+ and π^- before the collision. The directions and momenta have to be known only *after* the collision. The knowledge of the magnetic field topography is thus the only requirement necessary to reconstruct the collision vertex and to obtain the reaction energy, M_{+-}. Inelastic collisions are assumed to be negligible. Should there be a contribution from the G-parity violating process (electromagnetic) $\pi^+\pi^- \to \pi^+\pi^-\pi^\circ$, it could be detected by $\gamma\gamma$-conversion outside the pot. If two additional pions are produced ($\pi^+\pi^- \to \pi^+\pi^-\pi^\circ\pi^\circ$ or $2\pi^+\,2\pi^-$), of which only two charged pions are measured, the kinematic constraints can eliminate many possible misinterpretations of the event as an elastic one since the sum of the energies of two pions in this case should lie in the limits $400 < T_+ + T_- < 800$ MeV; if two pions are missing, it will be observed in the limits $100 < T_+ + T_- < 500$ MeV.

5.3. *Effective pion lifetime*

The formulae for luminosity [Eq. (21)] contain τ, the pion lifetime in the laboratory. Because of losses τ is not simply $\gamma\tau_0$. We now calculate the effective lifetime.

Pions will be lost from the hadron jumble not only by their natural decay but by their multiple traversals through the target. To estimate the amount of material seen we use the following simplified model. All orbits are tangent to the z axis, which goes through the center of the target. Due to the vertical free oscillations, the orbits uniformly populate (approximately), the vertical aperture. Thus, the average length, $\bar{S}$, of target traversed per orbit is

$$\bar{S} = \frac{w}{\Delta z}\,\bar{S}_{\text{proj}} \tag{39}$$

where Δz is the vertical aperture (4 cm), w the width of the target (0.2 cm) and $\bar{S}_{\text{proj}}$ the average projected length traversed if all orbits are projected onto the $z = 0$ plane (see Fig. 6). For a target of

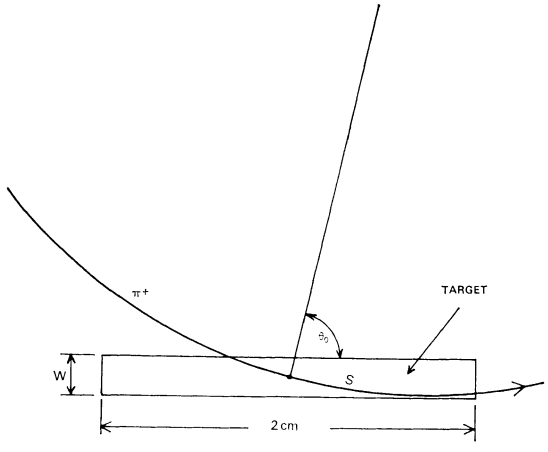

FIG. 6. Schematic showing amount of target material traversed by π^+ whose orbit lies in the midplane and whose orbit center lies on a line thru the target center which makes an angle of θ_0 with respect to the target.

thickness 2 cm in the beam direction and 0.2 cm wide square cross section we obtain $\bar{S}_{\text{proj}} = 0.5$ cm based on a calculation using the above model. Thus $\bar{S} = 0.025$ cm.

The traversal losses arise from three processes:

(a) Energy degradation. For the tungsten target described above 300 MeV π's will lose 100 MeV in 180 turns. This should be compared to the 115 turns they make in one laboratory lifetime.

(b) Multiple scattering. This will cause small losses. The total multiple scattering in 115 turns is 6°, while our vertical angular acceptance is around $\pm 10°$.

(c) Nuclear interaction. The interaction length in tungsten is 7.8 cm while 180 turns corresponds to 4.4 cm of traversal. From this we can see that collision losses will be as important as decay losses in limiting luminosity. Collision losses can be represented by a collision lifetime, τ_c, so that the effective τ_π is

$$\tau_{\text{eff}} = \frac{\tau_c \tau_\pi^{\text{LAB}}}{\tau_c + \tau_\pi^{\text{LAB}}}. \tag{40}$$

Traversal of 7.8 cm corresponds to 310 turns or about 2.5 natural lifetimes. Thus, $\tau_c \simeq 2.5\tau_\pi^{\text{LAB}}$ and

$$\tau_\pi^{\text{eff}} = 0.7\tau_\pi^{\text{LAB}}. \tag{41}$$

5.4. *Numerical examples for π–π collisions: Table I*

For the central target Precetron like the one in Fig. 4 we calculate the luminosity using Eq. (35), with $\bar{\lambda}$ given by (B.19) and $\bar{L}$ by (21) with τ given by (41); it is given by Eq. (10) with $R = 9.4$ cm ($\bar{R} = 6.6$ cm), $\eta = \frac{1}{2}$, $\kappa = (4.5)^{-1}$, $\Delta z = \pm 2$ cm, the latter satisfies our condition $(z/R)^2 < 1$ (see Appendix A) since $(\Delta z/R)^2 = (2/10)^2$. $n_+ = Nf_+$ is computed in Appendix C to be 1.8×10^{13}. G is given for the pulsed regime (Fig. 5) by Eq. (22a) and for nonpulsed regime by Eq. (22b). We have considered several cases of the time structure of the primary proton beam:

Without storage ring for the primary beam

Case A. Present LAMPF Structure: 120 pulses for second ($b = 120$) each 500 μsec long ($g = 8300$, with the effective laboratory pion lifetime taken to be 0.6×10^{-7} sec). Pulsed detectors—formula (22) used for G.

Case B. Same as *A* with detectors open all the time—formula (23) used for G.

Case C. Modulated Injection; instead of 120 pulses which are 500 μsec long, one has 2×10^5 pulses which are 0.06 μsec long ($g = 1$), i.e. each macropulse is modulated to produce one pulse

TABLE I

The π–π luminosity and interaction rate in the ρ-mass region in a central-target Precetron of radius 10 cm and pulsed $B = 400$ kG, with 1 mA protons incident on Tungsten target 2 cm thick. The μ–μ rates may be as much as 1 per cent of the π–π rates.

Configuration	Proton pulse length in units of pion lab. life-time g	No. of proton pulses per sec b	Time structure factor of proton beam, G [Eq. (22)]	No. of π^+ per sec for 2 cm of target (tungsten†) η^+	$\bar{L}$ Luminosity cm^{-2}/hr	I Inter-actions/hr
A. Present LAMPF structure, pulsed detectors	8300	120	1.2×10^{-10}	1.8×10^{13}	5×10^{19}	5×10^{-6}
B. Present LAMPF structure, nonpulsed detectors	8300	120	2×10^{-6}	1.8×10^{13}	8×10^{23}	8×10^{-2}
C. Modulated injection, pulsed detectors	1	2×10^5	5×10^{-6}	3.6×10^{12}	9×10^{22}	9×10^{-3}
D. P storage ring Store each macropulse, pulsed detectors	1	120	3.3×10^{-3}	1.8×10^{13}	1.4×10^{27}	140
E. H^- storage ring Store one macropulse, pulsed detectors	1	120	3.3×10^{-3}	1.8×10^{12}	1.4×10^{25}	1.4
F. P storage ring Store 120 macropulses, pulsed detectors	1	1	0.4	1.8×10^{13}	1.7×10^{29}	1.7×10^4
G. H^- storage ring Store 120 macropulses, pulsed detectors	1	1	0.4	1.8×10^{12}	1.7×10^{27}	170

† To obtain η_+ from a carbon target 2 cm thick, divide the numbers in this column by 7.77 and to obtain $\bar{L}$ and I, divide the numbers in the corresponding columns by 60.

which is one pion lifetime long, every four pion lifetimes. Pulsed detectors.

With storage ring for primary beam (see Sec. 2.4)

Case D. Store each macropulse for 500 μsec, then empty it onto Precetron target in 0.06 μsec ($g = 1$). Pulsed detectors.

Case E. Same as *D*, except that the H^- beam is stored, its intensity being 10 per cent that of the proton beam. Pulsed detectors.

Case F. Store protons for one second and dump them onto Precetron target in 0.06 μsec. Pulsed detectors.

Case G. The same as *F*, except that the H^- beam is stored, its intensity being 10 per cent that of the proton beam. Pulsed detectors. The numerical values for each case are given in Table I.

5.5. *Muon-muon collisions*

The lepton jumble. The solid metal target in the middle of the 'magnetic pot' will gradually (within a few effective π lifetimes) remove all undecayed hadrons by stopping them or by scattering them out. Only the muons from the pion decay and few electrons from the mu-decay will stay in orbit. The orbits will eventually pull away from the target, as shown in Fig. 7b. The mechanism by which the lepton orbits get detached from the target is the following: muons from π decay are generally emitted at an angle different from 0° with the pion direction (Fig. 7a). While the parent pion was heading toward the target at which it was created (Liouville's theorem), the muon direction is generally different and thus will *avoid* the target. The exception is when the decay takes place too close to the target to escape it. A large fraction of the muons will miss the target and continue orbiting in a new phase space. The muons that hit the target will continue traversing it until all their energy is lost.

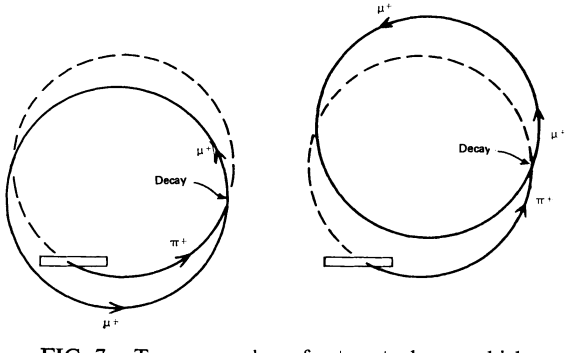

FIG. 7a. Two examples of $\pi^+ - \mu^+$ decay which produce μ^+ orbits which will never hit the target.

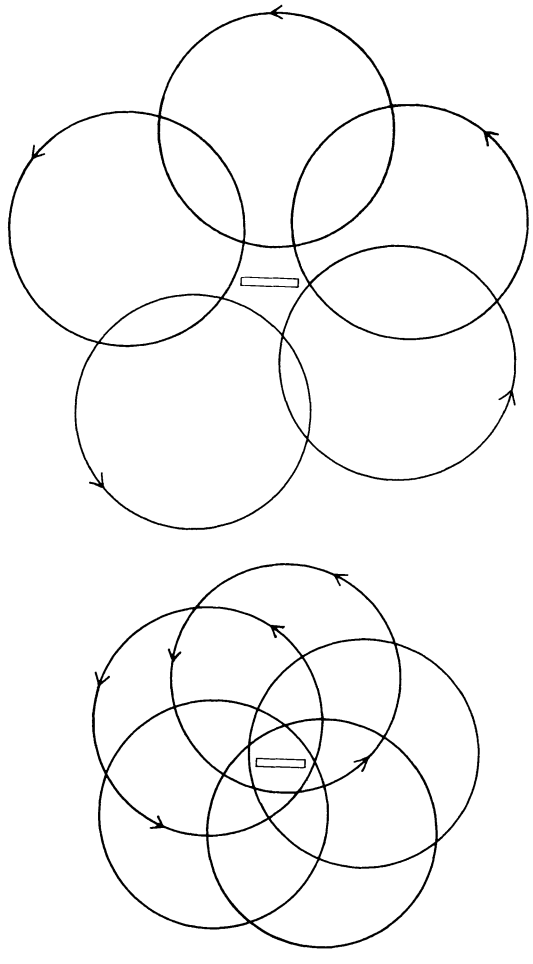

FIG. 7b. Families of orbits corresponding to the two examples of decay in Fig. 7a.

Muon-muon luminosity and reaction rate. Because the μ's have a much longer lifetime than the π's, Eq. (35) is approximately valid for the muon rate as well. For the μ's that orbit without hitting the target the μ lifetime is about 100 times that of the π's. Here we can use lower instantaneous rates because $g = 1$ now means a 10 μsec proton pulse. The luminosity then would go up by a factor of the order of 100 if all the μ's were captured in orbits that miss the target. We have not calculated the fraction of μ's that are captured in orbits that avoid the target. However, on the basis of our qualitative discussion of Fig. 7 we would expect a reasonable fraction to avoid the target.

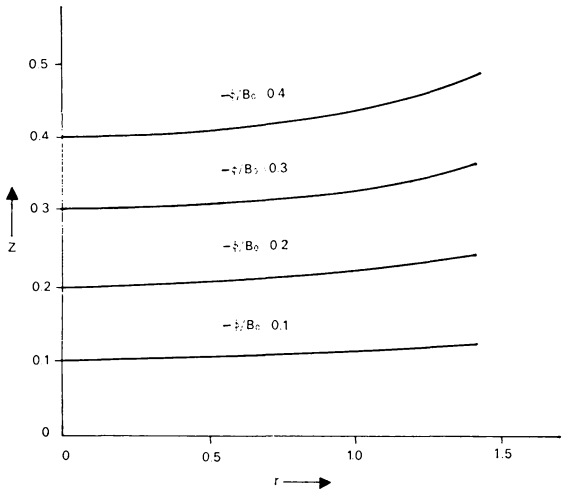

FIG. 8. Equipotential surfaces for the case $k=0.1$ and $R=1.0$.

Since the μ–μ interaction is a second-order electromagnetic process, one would expect the μ–μ cross sections to be about 10^4 times smaller than the π–π cross sections. Thus the μ–μ collision rates will probably be at least a factor of 100 lower than the π–π collision rates given in Table I.

5.6. *Limitations*

We enumerate and comment on some important approximations of our calculations as well as some practical limitations of our 'Precetron' model:

1. Collective phenomena such as space-charge effects, beam-beam interactions, etc. have been neglected in our treatment of orbits. Only single particle orbits were computed and then only to first order.

2. A 400 kG field in the volume required is yet to be accomplished. However, it has been achieved[8] in a $\frac{5}{8}$ in. bore.

3. The 0.2 cm diameter, 2 cm long tungsten target in our numerical example must dissipate around 50 kW of power. At LAMPF a 1 cm diameter, 10 cm long graphite target has been stably operated while dissipating 62 kW. At incipient burn-out this target was receiving 94 kW.[9]

4. Radiation damage to the coils of this device may be a problem but it is a common problem to the thick target facilities of meson factories.

5. The background from the π collisions with the target and the gas in the vacuum system (assuming 10^{-8}) will exceed the number of π–π collisions by orders of magnitude, but no charged reaction product can come out of the magnetic field, except those which change their direction. Thus, the main background will be photons and neutrons. The study of the methods for discriminating the π–π collisions from the background is beyond the scope of this article.

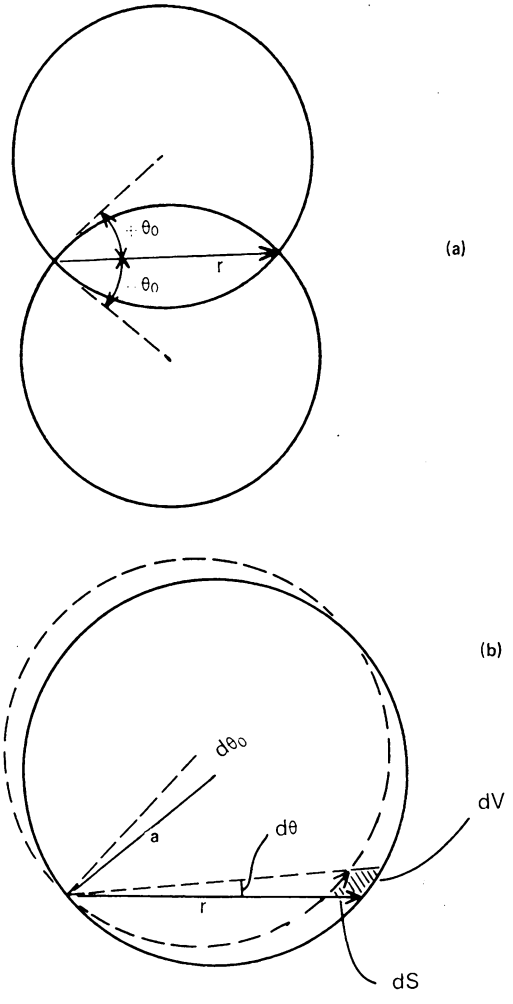

FIG. 9. (a) Two orbits at $\pm\theta_0$ passing through point r; (b) Orbits defining dV; dS is the *arc* length of the dashed orbit.

6. OFFSET PRECETRON

In Fig. 10 we show a Precetron configuration which looks like a colliding beam device. It has the target offset from the center of symmetry. We consider the case where orbits are confined to a shell between ηR and R and the orbits enclose the center of symmetry of the field. The target is located at

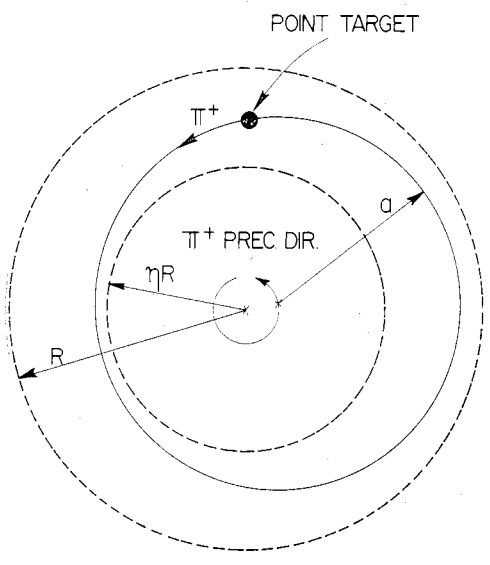

FIG. 10. Offset Precetron. The π-producing target is located in the middle of the peripheral zone defined by the radii ηR and R. For $\eta \to 1$, we have 'colliding beams' in Fig. 3. For $\eta \to 0$, we have the opposite extreme: large angular acceptance and significant precession, i.e. the 'self-colliding orbits'. The acceptance is calculated in Sec. 6.

$(1+\eta)R/2$, i.e., in the middle of the shell. The angular acceptance of this configuration for sizable values of $(1-\eta)$ is large but obviously not as large as for the central Precetron. In order to produce comparable π^+ and π^- densities one would need either to use one beam with $\sim 90°$ production (Fig. 3a) or two proton beams where one captures forward production (Fig. 3b).

From the geometry in Fig. 10 we can calculate the horizontal angular acceptance. It clearly depends upon the particle momentum. For a fixed momentum p which has a corresponding radius of curvature, r, in the Precetron field the angular acceptance is:

$$\text{Acceptance} = 2\cos^{-1}\left\{1 - \frac{(1-\eta)}{2(1+\eta)r} \cdot [(1-\eta)R - 2\,|\,2r-(1+\eta)R\,|\,]\right\} \quad (42)$$

where the range of r is given by

$$\left(\frac{1+3\eta}{4}\right) R < r < \left(\frac{3+\eta}{4}\right) R \quad (43)$$

For small values of $x = (1-\eta)$ it is approximately:

$$\text{Acceptance} = \sqrt{x[x - 2\,|\,2r/R - 2 + x\,|\,]} \quad (44)$$

For $\eta = \frac{1}{2}$ and $r = [(1+\eta)/2]R = \frac{3}{4}R$ the acceptanc from Eq. (42) is 0.9 radians.

For $\eta = \frac{3}{4}$ and $r = [(1+\eta)R]/2 = \frac{7}{8}R$ the acceptanc from Eq. (42) is 0.4 radians.

For $(1-\eta)$ small, the particle density of thi configuration will be approximately uniform an $\bar{\lambda}$ of formula (35) is unity.

The momentum acceptance of this configuratio is limited to the momenta corresponding to radii

$$r = \left(\frac{1+\eta}{2}\right) R \pm \left(\frac{1-\eta}{4}\right) R \quad (4$$

or a

$$\frac{\Delta p}{p} \text{ of } \pm \tfrac{1}{2}\left(\frac{1-\eta}{1+\eta}\right) \quad (4$$

For $\eta = \frac{1}{2}$ the full momentum bite is $\frac{1}{3}$, for $\eta =$ it is $\frac{1}{7}$. Thus it can be seen that the offset Precetro with $(1-\eta) \sim \frac{1}{2}$ will have a luminosity approachin that of the central Precetron providing one use two proton beams to fill it.

By setting $\eta = 0$, Eqs. (42) and (45) give th acceptance for all momenta larger than th momentum corresponding to a radius of curvatur $R/4$.

APPENDIX A

Precetron orbits

In this section we calculate single particle orbi for cylindrically symmetric fields which fall o weakly with radius. We show that the orbi precess, that the vertical oscillations are stable an we calculate the vertical acceptance.

An exact solution of Maxwell's equations (i cylindrical coordinates) which possesses focussin properties is

$$B_\theta = 0 \quad \text{(a)}$$

$$B_r = \frac{-2k}{R^2} B_0 rz \quad \text{(b) (A.}$$

$$B_z = B_0\left[1 - \frac{kr^2}{R^2} + \frac{2kz^2}{R^2}\right] \quad \text{(c)}$$

where k and R are constants. The constant R introduced to make k dimensionless and will t taken as a radius characteristic of the dimension the magnetic 'pot'.

If k is small the field is nearly uniform and th orbits approximately circular. The average valu of 'n' for orbits of radius a passing through th center of symmetry is given below lowest order i k as

$$= \frac{1}{2\pi a}\int_{\text{orbit}} \frac{-r(\partial B_z/\partial r)\mathrm{d}s}{B_z} \simeq \frac{1}{\pi a}\int_{\text{orbit}} \frac{kr^2}{R^2}\,\mathrm{d}s$$
$$= \frac{4ka^2}{R^2} \qquad \text{(A.2)}$$

For the largest diameter orbit the radius is $R/2$ ince

$$\bar{n} = k \qquad \text{(A.3)}$$

From betatron theory we expect no difficulty aintaining stable vertical oscillations if $\bar{n} < 1$.

The field given above for small k, can be proximately achieved around the midpoint of two entical coils of radius, a, separated by a distance, l, $\mathrm{d} \neq a$. The first few terms in an expansion of , in terms of z/a and r/a are[10]

$$B_d = \frac{\mu I}{a}\sin\alpha\left[P_1{}^1(\cos\alpha) + P_3{}^1(\cos\alpha)\,\frac{2z^2-r^2}{2a^2} + P_5{}^1(\cos\alpha)\,\frac{(8z^4-24z^2r^2+3r^4)}{8a^4}\right] + \ldots \qquad \text{(A.4)}$$

here P_n^1 are the associated Legendre functions and n $\alpha = a/\mathrm{d}$. The corresponding expansion for B_r

$$= -\left(\frac{\mu I}{a}\sin\alpha\right)\left[P_3{}^1(\cos\alpha) + \frac{(4z^2-3r^2)}{2a^2} \cdot P_5{}^1(\cos\alpha)\right]\left(\frac{rz}{a^2}\right) \qquad \text{(A.5)}$$

y using two sets of coils each set of different radii, parations, and currents, it is possible to choose ese parameters to obtain any desired value for e ratio of coefficients of second order to zeroth der terms and at the same time make the fourth der term vanish. Thus, departures from q. (A.4) comes in only at sixth order and higher. learly, by a suitable arrangement of sets of coils varying radii and separations, one can approxiate (A.1) as closely as is needed.

The field given by (A.1) can be obtained from a alar potential, ϕ, given by

$$\phi(r, z) = -B_0 z\left(1 - \frac{kr^2}{R^2} + \frac{2kz^2}{3R^2}\right) \qquad \text{(A.6)}$$

he equipotential surfaces of (A.6) give rise to the llowing family of curves in ϕ = const. planes:

$$r^2 = \frac{R^2}{k}\left(\frac{\phi}{B_0 z} + \frac{2kz^2}{3R^2} + 1\right) \qquad \text{(A.7)}$$

hese are shown graphically in Fig. 8 for a typical se $k = 0.1$ and $R = 1$. One could also achieve .1) by suitably shaped iron pole tips in a magnet.

The equations of motion for $B_\theta = 0$ in cylindrical coordinates are

$$m\ddot{r} = mr\dot{\theta}^2 + (e/c)r\dot{\theta}B_z \qquad \text{(a)}$$
$$\frac{\mathrm{d}}{\mathrm{d}t}(mr^2\dot{\theta}) = \frac{er}{c}(\dot{z}B_r - \dot{r}B_z) \qquad \text{(b)} \quad \text{(A.8)}$$
$$m\ddot{z} = -\frac{er}{c}\dot{\theta}B_r \qquad \text{(c)}$$

where $m = m_0\sqrt{1-\beta^2}$ and $\beta = v/c$ = constant for static fields. Eq. (A.8b) can be integrated once to give using the initial condition $r(0) = 0$

$$\dot{\theta} = \frac{\omega_0}{2}\left(1 - \frac{kr^2}{2R^2} + \frac{2kz^2}{R^2}\right) \qquad \text{(A.9)}$$

where $\omega_0 = -eB_0/\mathrm{cm}$.

Substituting (A.9) for $\dot{\theta}$ yields the following coupled equations for r and z:

$$\ddot{z} = -\omega_0^2\frac{k}{R^2}\cdot r^2 z\left(1 - \frac{kr^2}{2R^2} + \frac{2kz^2}{R^2}\right) \qquad \text{(a)}$$
$$\ddot{r} = -\frac{r\omega_0^2}{4}\left[1 - \frac{2kr^2}{R^2} + \frac{4kz^2}{R^2} + \frac{k^2}{R^4}\left(\frac{3r^4}{4} - 4z^2r^2 + 4z^4\right)\right] \qquad \text{(b)} \quad \text{(A.10)}$$

We shall take initial conditions as

$$r(0) = z(0) = \theta(0) = 0$$
$$\dot{r}(0) = v_r \neq 0 \qquad \text{(A.11)}$$
$$\dot{z}(0) = v_z \neq 0$$

For k = 0, the motion is simple, i.e.,

$$\theta = \omega_0 t/2$$
$$r_0 = 2a\sin\theta$$
$$z_0 = \dot{z}(0)t \qquad \text{(A.12)}$$
$$\omega_0 = eB_0/mc$$
$$a = v_r/\omega_0$$

These are helical orbits whose motion in z = constant planes are circular orbits. If we now consider k and z^2/R^2 as small quantities and expand (A.9) and (A.10), keeping only lowest order terms, we have

$$\ddot{z} = -\omega_0{}^2\frac{k}{R^2}r^2 z \qquad \text{(a)}$$
$$\ddot{r} = -\frac{r\omega_0{}^2}{4}\left(1 - \frac{2kr^2}{R^2}\right) \qquad \text{(b)} \quad \text{(A.13)}$$
$$\dot{\theta} = \frac{\omega_0}{2}\left(1 - \frac{kr^2}{2R^2}\right) \qquad \text{(c)}$$

Eq. (A.13b) has solutions in terms of Jacobian elliptic functions.

$$\mathrm{Sn}\left(\frac{\omega_0 t}{2\sqrt{m^2+1}} \mid m^2\right) \qquad \text{(A.14)}$$

where

$$m^2 = \frac{1-\sqrt{1-4k'}}{2k'} - 1 \qquad k' = (2a/R)^2 k \tag{A.15}$$

This can be seen by integrating (A.13b) once using the substitution $\dot{r} = P$ and obtaining

$$\dot{r}^2 = v_r^2 - \frac{\omega_0^2}{2}\left(\frac{r^2}{2} - k\,\frac{r^4}{2R^2}\right) \tag{A.16}$$

Using $v_r^2 = \omega_0^2 a^2$, (A.16) becomes

$$\dot{r} = \omega_0 a\sqrt{1-(r/2a)^2 + k'(r/2a)^4} \tag{A.17}$$

Integrating (A.17) once leads to

$$\frac{\omega_0 t}{2\sqrt{m^2+1}} = \int_0^u \frac{\mathrm{d}u}{\sqrt{(1-u^2)(1-m^2u^2)}} \tag{A.18}$$

where

$$u = \frac{r}{2a\sqrt{m^2+1}} \tag{A.19}$$

and

$$m^2 = \frac{1-\sqrt{1-4k'}}{2k'} - 1 \tag{A.20}$$

Eq. (A.18) is a standard elliptic integral defining the Sn function.[11]

Therefore, the solution of (A.13b) is

$$r = 2a\sqrt{m^2+1}\,\mathrm{Sn}\left(\frac{\omega_0 t}{2\sqrt{m^2+1}} \mid m^2\right). \tag{A.21}$$

An expansion of (A.21) to first order in k' yields[12]

$$r = (2a)\left(1+\frac{9}{16}k'\right)\left(\sin\alpha t + \frac{k'}{16}\sin 3\alpha t\right) \tag{A.22}$$

where

$$\alpha = \frac{\omega_0}{2}\left(1-\frac{3k'}{4}\right). \tag{A.23}$$

Using Eq. (A.22) for r, we obtain, to first order in k', the following relationship:

$$\theta = \int_0^t \dot{\theta}\,\mathrm{d}t = \frac{\omega_0}{2}[(1-k'/4)\,t + (k'/8\alpha)\sin 2\alpha t]. \tag{A.24}$$

We can use (A.24) to eliminate t from (A.22) and obtain $r(\theta)$. Carrying this out to first order in k' results in

$$r = 2a(1+k'/2)\sin\theta(1-k'/2). \tag{A.25}$$

From (A.25) we deduce that the orbits precess about the z axis with a period $4/k'$ times the orbital period. In one orbital period the angle changes by $\Delta\theta = \pi k'/2$. Thus, the number of orbital period required for one precessional period is

$$2\pi/\Delta\theta = 4/k'. \tag{A.26}$$

The solution (A.22) can now be inserted into Eq. (A.10a) to obtain an equation for the z motion. Thus,

$$\ddot{z} = -\omega_0^2 k' z \sin^2\alpha t \tag{A.27}$$

or

$$\ddot{z} + \frac{\omega_0^2}{2}k'(1-\cos 2\alpha t) \quad t = 0 \tag{A.28}$$

Eq. (A.28) is in the standard form for Mathieu equation and possesses a Floquet solution, which for small k is[13]

$$z(t) = \frac{\dot{z}(0)}{v_r}\sqrt{\left(\frac{2}{k'}\right)}\frac{a}{(1-k'/2)}\left(\sin\frac{\omega_0}{2}\sqrt{2k'}\,t\right) \cdot\left(1-\frac{k'}{2}\cos 2\alpha t\right). \tag{A.29}$$

Thus, the vertical oscillations are stable with amplitudes, S, given by

$$S = S_0\sqrt{\frac{2}{k'}}\,\frac{a}{(1-k'/2)} \tag{A.30}$$

where S_0 is $\dot{z}(0)/v_r$, the initial slope in a vertical plane containing the z axis. Let $h = \Delta z/2$ be the vertical half aperture, then the maximum acceptable slope is

$$S_{\max} = \frac{h}{a}\sqrt{\left(\frac{k'}{2}\right)}(1-k'/2) = \frac{\Delta z}{R}\sqrt{\frac{k}{2}}\left(1-\left(\frac{2a}{R}\right)\frac{k}{2}\right) \simeq \frac{\Delta z^2 k}{R\;2}\sqrt{\frac{k}{2}}. \tag{A.31}$$

APPENDIX B

Precetron particle density calculations

We wish to calculate the particle density, ρ, for δ function orbit diameter, x, distribution. We assume a uniform distribution for z and θ_0, where θ_0 is the angle of the orbit center in cylindrical coordinates. Clearly, ρ is a function of r only hence we will set $\theta = 0$. As shown in Fig. 9a, two orbits pass through each given point, (r, θ). The density ρ is defined by

$$\rho(r)\,\mathrm{d}V = \rho(r) r\,\mathrm{d}r\,\mathrm{d}\theta\,\mathrm{d}z = \text{number of particles in d} = 2\left(\frac{N_T}{2\pi\Delta z}\,\mathrm{d}\theta_0\,\mathrm{d}z\right)\left(\frac{\mathrm{d}S}{2\pi a}\right). \tag{B.}$$

The factor 2 is present because of the two orbits $\pm\theta_0$. The first factor in parenthesis is the numb

If orbits around θ_0 which pass through dV as shown on Fig. 9b; and the second factor is the fraction of each orbit in dV. N_T is the total number of particles considered.

Now $r = 2a\cos\theta_0$, and

$$dS = \frac{r\,d\theta}{\cos\theta_0} = 2a\,d\theta. \tag{B.2}$$

Hence,

$$\rho(r)\,dV = \frac{N_T}{\pi^2(\Delta z)}\,d\theta_0\,dz\,d\theta = \rho(r)r\,dr\,d\theta\,dz \tag{B.3}$$

and

$$\rho(r) = \frac{N_T}{\pi^2(\Delta z)r}\frac{\partial(\theta_0,\theta,z)}{\partial(r,\theta,z)} = \frac{N_T}{\pi^2(\Delta z)r\sqrt{4a^2-r^2}} \tag{B.4}$$

where the Jacobian is

$$\left|\frac{dr}{d\theta_0}\right|^{-1} = \frac{1}{\sqrt{4a^2-r^2}}. \tag{B.5}$$

Letting $x = 2a$, we have

$$\rho(r,x) = \frac{N_T}{\pi^2\Delta z}\cdot\frac{1}{\sqrt{x^2-r^2}}\cdot\frac{1}{r}. \tag{B.6}$$

The density, ρ, is normalized to N_T, the total number of particles, as the integral below shows:

$$\int_{\text{pot}}\rho(r)r\,dr\,d\theta\,dz = N_T. \tag{B.7}$$

If we now take an x distribution, $f(x)$, corresponding to some momentum distribution, then the π^+ particle density, $D_+(\mathbf{r})$ is given by

$$D_+(r,\theta,z) = N_+\int_r^R \frac{f(x)\,dx}{\pi^2(\Delta z)r\sqrt{x^2-r^2}} = D_+(r) \tag{B.8}$$

where N_+ is the total number of orbiting π^+'s. The luminosity is then determined from

$$L = \int_{\text{vol. of shell}} 2D_+D_-\beta_{12}c\,dV. \tag{B.9}$$

For a uniform x distribution in a shell from ηR to R we have

$$f(x) = \frac{1}{(1-\eta)R} \quad \eta R \leqslant x \leqslant R \tag{B.10}$$

and D_+ becomes

$$D_+(r) = \frac{N_+}{1-\eta}\frac{1}{\pi^2R(\Delta z)r}\,\text{sech}^{-1}\frac{r}{R}. \tag{B.11}$$

Using this in (B.9) yields

$$\bar{L} = \left(\frac{2\beta_{12}c\kappa N_+^2}{\pi R^2\Delta z(1-\eta^2)}\right)\bar{\lambda}^2 \tag{B.12}$$

$$\bar{\lambda}^2 = \left(\frac{1-\eta}{1+\eta}\right)\frac{2}{\pi^2}\int_\eta^1\frac{dx}{x}(\text{sech}^{-1}x)^2. \tag{B.13}$$

If we take $n = \frac{1}{2}$, then $\bar{\lambda} \simeq 0.58$.

The actual π^+ momentum distribution is not uniform and will modify the results above. A convenient polynomial approximation for $f(x)$ corresponding to the π^+ spectrum expected from 800-MeV protons[14] on tungsten is

$$f(x) = \frac{12}{R}\left(\frac{x}{R}\right)^3\left[1-\frac{x}{R}^2\right]\ 0 \leqslant x \leqslant R. \tag{B.14}$$

R is the maximum diameter orbit. The distribution (B.14) yields an average value, $\bar{x}$ given by

$$\bar{x} = \bar{R} = 0.69R \tag{B.15}$$

and, a variance σ_x of

$$\sigma_x = 0.35\bar{R} = 0.25R. \tag{B.16}$$

Using (B.14) we obtain

$$D_+ = \frac{8}{5\pi^2}\frac{N_+}{R(\Delta z)r}\left(1-\frac{r^2}{R^2}\right)^{3/2}\left(1+\frac{4r^2}{R^2}\right). \tag{B.17}$$

Computing $\bar{L}$ using (B.17) and (B.9) results in

$$\bar{L} = \left(\frac{2\beta_{12}c\kappa N_+^2}{\pi(\Delta z)R^2(1-\eta^2)}\right)\bar{\lambda}^2 \tag{B.18}$$

where

$$\bar{\lambda}^2 = \frac{128}{25\pi^2}(1-\eta^2)\int_\eta^1\frac{dy}{y}(1-y^2)^3(1+4y^2)^2. \tag{B.19}$$

If $\eta = \frac{1}{2}$, then $\bar{\lambda} = 0.85$.

APPENDIX C

Pion production with 800 MeV *protons*

According to LAMPF studies (p. 29 of Ref. (1)), a 1-mA average proton beam (6×10^{15} p/s) of 800 MeV incident upon 18 grams/cm^2 Be target will yield, at 15°, 1.1×10^{10} π^+/sec (with T_π = 300 MeV, in a channel with the momentum and solid angle acceptances Δp = 6.7 per cent, $\Delta\Omega = 3\times10^{-3}$) at 43 ft from the production point (the decay length is 74.6 ft). From this we compute the pion yield per 1 mA of protons, Y, per 1 cm thickness of Be target per sr/MeV/c to be:

$$n_+ = fN = 2.36\times10^{10}\,\Delta\Omega\,\Delta p(\pi^+/\text{sec/cm} \cdot \text{Be/sr/MeV/c/1mA protons}) \tag{C.1}$$

Scaling this by $(A_{Be}/A_w)^{1/3}$ to obtain a tungsten yield gives

$$n_+ = fN = 9.1 \times 10^{10}\, \Delta\Omega\, \Delta p(\pi^+/\text{sec/cm} \cdot \text{W/sr/MeV/c/1mA protons}) \quad \text{(C.2)}$$

Assuming that the π-production cross section is constant out to 45° and then drops abruptly to zero, we obtain an effective solid angle of 0.45 steredians for the Precetron. We assume $\Delta z = \pm 2$ cm which gives $\Delta\phi = \pm 0.15$ (use formula A.31) and $\Delta\theta = \pm 180°$.

We take a momentum bite of

$$\frac{\Delta p\pi}{p\pi} = 0.5 \quad \text{(C.3)}$$

full width at $p_\pi = 415$ MeV/c, which corresponds approximately to the ρ-meson mass region ($m_\rho = 765$ MeV). With these parameters $n_+ = 1.8 \times 10^{13}$ for a tungsten target 2 cm long.

ACKNOWLEDGEMENTS

We are particularly thankful to Kenneth Robinson for his most valuable explanations, discussions and important suggestions used in this study, and to Stanley Livingston for his hospitality and discussions during the stay of one of us (B.M.) at the Cambridge Electron Accelerator as visiting scientist.

We are indebted to Gerald O'Neill, D. Nagle, Ernest Courant,[15] and Edwin McMillan for their most useful discussions and encouraging attitudes to our idea of π–π collisions.

REFERENCES

1. (a) A Proposal for a High Flux Meson Physics Facility ('LAMPF') (800 MeV), Los Alamos Scientific Laboratory Report, Sept. 1964 (not numbered); (b) L. Rosen, 'Meson Factories', *Phys. Today*, **19,** 21 (1966); (c) D. C. Hagerman, *IEEE Trans. Nucl. Sci.*, **NS-13,** 277 (Aug. 1966). The recent progress report on all meson factories (1–4) can be found in *Proceedings of 1969 Int. Conf. on H.E. Nuclear Physics at Columbia University, N.Y.* (Plenur Press, N.Y. 1970).
2. Isochronous Ring Cyclotron (580 MeV), Swiss Institut for Nuclear Research, Zurich; see: J. P. Blaser and H. O. Willax, *IEEE Trans. Nucl. Sci.*, **NS-13,** 19 and 451 (Aug. 1966).
3. Tri-University Meson Facility (500 MeV) ('TRIUMF')– (a) 'Proposal and Cost Estimates', edited by E. W Vogt and J. J. Burgerjon, University of Britis Columbia, Vancouver, B.C., Nov. 1966; (b) E. W Vogt and J. R. Richardson, *IEEE Trans. Nucl. Sci* **NS-13,** 262 and 426 (Aug. 1966).
4. Spiral Ridged Cyclotron (700 MeV), Dubna: V. F Dmitrievsky, V. P. Dzelepov, V. V. Kolga, an V. I. Zamolodchikov, *IEEE Trans. Nucl. Sci* **NS-13,** 215 and 512 (Aug. 1966).
5. P. L. Csonka and A. M. Sessler, ISR/CERN Repor PS/5977/EEK and ISR/TH-67-29 (1967). (Se remark under Ref. (6).)
6. P. L. Csonka, CERN Yellow Report 67-30 and CERN TH-836 (1967). In these reports, as well as i Ref. (5), the $\pi\pi$ collision rates are calculated on th assumption that the $\pi\pi$ luminosity is proportiona to the square of the pion lifetime, $\tau_\pi{}^2$; this should b compared to our formula (17) which shows the τ_π dependence for the integrated luminosity.
7. The early version of this paper entitled 'Precetron— principle for obtaining pion-pion and muon-muo collisions' by R. Macek and B. Maglic appeared a Princeton–Pennsylvania Accelerator Report PPAR 14 (June 24, 1969).
8. S. Foner, National Magnet Laboratory, MIT (privat communication).
9. D. R. F. Cochran, *Proc. 2nd LAMPF Users Meetin 1969*, Los Alamos Scientific Laboratory Repor LA-4087-MS, p. 23.
10. D. R. Smythe, *Static and Dynamic Electricity*, p. 27 (McGraw-Hill, N.Y., 1950).
11. J. Matthews and R. Walker, *Mathematical Methods c Physics*, p. 196 (W. A. Benjamin, Inc., N.Y., 1964) also chapters 16 and 17 in Ref. (12).
12. M. Abramovitz and I. Stegun, *Handbook of Mathematic Functions*, National Bureau of Standards (U.S Government Printing Office, Washington, D.C 1965), p. 575, Eq. (16.23.1), and p. 591.
13. A. Erdelyj, Editor, *Higher Transcendental Function* Vol. 3, pp. 97 and 105 (McGraw-Hill, N.Y., 1955).
14. Equation (B.14) is a reasonable approximation to π spectrum shown on p. 35 of Ref. (1a).
15. E. D. Courant has pointed out to us that our collidin orbits were *self*-colliding, which we have no incorporated into the name.

Received 17 February 1970